Asiaticoside suppresses cell proliferation by inhibiting the NF-κB signaling pathway in colorectal cancer

XIN ZHOU[1*], CHUNLIN KE[2*], YOU LV[1*], CAIHONG REN[3*], TIANSHENG LIN[1], FENG DONG[2] and YANJUN MI[4]

[1]Department of Colorectal Cancer, Cancer Center, The First Affiliated Hospital of Xiamen University, Teaching Hospital of Fujian Medical University, Xiamen, Fujian 361003; Departments of [2]Radiotherapy and [3]Pathology, The First Affiliated Hospital of Fujian Medical University, Fuzhou, Fujian 350005; [4]Department of Medical Oncology, Xiamen Key Laboratory of Antitumor Drug Transformation Research, The First Affiliated Hospital of Xiamen University, Teaching Hospital of Fujian Medical University, Xiamen, Fujian 361003, P.R. China

Received February 7, 2020; Accepted June 11, 2020

DOI: 10.3892/ijmm.2020.4688

Abstract. Colorectal cancer (CRC) is one of the leading causes of cancer-associated mortality. Asiaticoside (AC) exhibits antitumor effects; however, to the best of our knowledge, the biological function of AC in CRC cells remains unclear. Therefore, the aim of the present study was to investigate the effect of AC on CRC cells. In the present study, CCK-8 and colony formation assays were performed to assess the effects of AV on human CRC cell lines (HCT116, SW480 and LoVo). Mitochondrial membrane potential was examined by JC-1 staining. Cell apoptosis and cell cycle were monitored by flow cytometry, and the expression of genes was evaluated using RT-qPCR and western blot analysis. Furthermore, the biological effect of AC *in vivo* was detected using a xenograft mouse model. The findings revealed that 2 μM AC suppressed the proliferation of CRC cells in a time- and dose-dependent manner, but had no adverse effects on normal human intestinal FHC cells at a range of concentrations. AC decreased the mitochondrial membrane potential and increased the apoptosis of CRC cells in a dose-dependent manner. Furthermore, AC induced cell cycle arrest at the G0/G1 phase. AC attenuated IκBα phosphorylation in a dose-dependent manner, thereby preventing P65 from entering the nucleus, and resulting in inhibition of the NF-κB signaling pathway. In addition, AC significantly reduced the expression of CDK4 and Cyclin D1 in a dose-dependent manner, significantly upregulated the activation of caspase-9 and caspase-3, and decreased the Bcl-2/Bax mRNA ratio. Furthermore, treatment with the NF-κB signaling pathway inhibitor JSH-23 significantly increased the cytotoxicity of AC in CRC cells. Findings of the xenograft mice model experiments revealed that AC significantly inhibited colorectal tumor growth in a dose-dependent manner. Overall, AC suppressed activation of the NF-κB signaling pathway by downregulating IκBα phosphorylation. This resulted in inhibition of CRC cell viability and an increase of cell apoptosis, which may form the basis of AC use in the treatment of patients with CRC.

Correspondence to: Dr Yanjun Mi, Department of Medical Oncology, Xiamen Key Laboratory of Antitumor Drug Transformation Research, The First Affiliated Hospital of Xiamen University, Teaching Hospital of Fujian Medical University, 55 Zhenhai Road, Xiamen, Fujian 361003, P.R. China
E-mail: mymiyanjun@163.com

Dr Chunlin Ke, Department of Radiotherapy, The First Affiliated Hospital of Fujian Medical University, 20 Chazhong Road, Fuzhou, Fujian 350005, P.R. China
E-mail: ke_chunlin@yeah.net

*Contributed equally

Key words: asiaticoside, NF-κB pathway, colorectal cancer, cell proliferation

Introduction

Colorectal cancer (CRC) was the third most common cancer and the third most common cause of cancer-associated mortality in 2019 in the USA (1). Patients with stage I and II CRC who undergo colectomy, proctectomy or proctocolectomy often receive neoadjuvant radiation or chemotherapy treatments to lower the risk of recurrence, whereas patients with stage III and IV CRC are typically treated with chemotherapy or radiotherapy (2). However, studies have suggested that drug resistance developed by patients with CRC limits the therapeutic efficacy of anticancer agents (3,4). Therefore, developing novel effective chemotherapy drugs will benefit patients with CRC.

Centella asiatica, a herb of the apiaceae family (5), contains a variety of active ingredients, such as triterpenoids and saponins (6). AC and madecassoside are the principal monomer components of saponins in *C. asiatica* (7). Previous studies have revealed that AC possesses a wide range of biological functions, such as facilitating angiogenesis by increasing collagen synthesis (8,9), inhibiting inflammatory process (10,11), suppressing scar formation (12,13) and promoting wound healing (12,13). Additionally, AC has a crucial function in inflammatory lung diseases (14), neurological disorders (15) and osteogenic differentiation of human

periodontal ligament cells (16). The clinical applicability of AC in the treatment of malignant tumors has been extensively studied over the last few years. Studies have confirmed that AC has a particular therapeutic effect on breast cancer (17), multiple myeloma and other tumors (18), and can improve the sensitivity of cancer cells to chemotherapy drugs (18,19). However, to the best of our knowledge, the biological function of AC in CRC cells remains largely unknown.

AC reduces the incidence of DMBA-induced breast cancer in rats by inhibiting expression of TNF-α and IL-1β (20). AC treatment considerably suppresses the proliferation of human breast cancer MCF-7 cells, and induces cell apoptosis *in vitro* (17). A previous study on multiple myeloma cancer cells indicated that AC inhibits cellular proliferation by inducing autophagy coupled with elevated expression of LC3-II (18). Notably, AC increases sensitivity of tumor cells to vincristine by promoting apoptosis and inducing cell cycle arrest (19).

Therefore, the aim of the present study was to improve understanding of the biological effects of AC on CRC cells. Using several functional experiments *in vitro* and in mice models *in vivo*, the present findings revealed that AC could inhibit activation of the NF-κB signaling pathway by suppressing IκBα phosphorylation, which may be one of the primary mechanisms of AC-induced CRC cell apoptosis and cell cycle arrest. Overall, the present data suggest that AC exhibits antitumor effects in CRC.

Materials and methods

Cell culture and solution preparation. Normal human intestinal FHC cells and human CRC cell lines (HCT116, SW480 and LoVo) were obtained from the Cell Bank of Shanghai Institutes for Biological Sciences, Chinese Academy of Sciences. The cells were cultured in Dulbecco's modified Eagle's medium (Hyclone; GE Healthcare Life Sciences) supplemented with 10% fetal bovine serum (Gibco; Thermo Fisher Scientific, Inc.) and 1% penicillin-streptomycin (Gibco; Thermo Fisher Scientific, Inc.) in an incubator at 37˚C, containing 5% CO_2. Culture medium was changed every 24 h.

A total of 95.90 mg AC (Santa Cruz Biotechnology, Inc.) was weighed and dissolved in 100 μl dimethyl sulfoxide (DMSO; Santa Cruz Biotechnology, Inc.) to prepare a 1 mM storage solution. Subsequently, different concentrations of the working solutions (0.1, 0.5 and 2 μM) were prepared using culture medium. Cells at the logarithmic growth phase were treated with the working solutions. A quantity of 0.2% DMSO was used as the control.

Cell Counting Kit-8 (CCK-8) assay. Cell viability was assessed using a CCK-8 assay. CRC cells and FHC cells in the logarithmic growth phase were digested and seeded into 96-well plates at a density of $5x10^3$ cells/well followed by treatment with various concentrations of AC (0.1, 0.5 and 2 μM) at 37˚C. Cells treated with 0.3% DMSO were used as the negative controls. Subsequently, 10% CCK-8 reagent (Beijing Zoman Biotechnology Co., Ltd.) was added to each well at different time intervals (24, 48 and 72 h), and cells incubated for 2 h at 37˚C. The absorbance was then measured using a microplate reader (Bio-Rad Laboratories, Inc.) at a wavelength of 450 nm.

Colony formation assay. CRC cells in the logarithmic growth phase were seeded in 6-well plates ($1x10^3$ cells/well) and then treated with different concentrations of AC (0.1, 0.5 and 2 μM) at 37˚C. After 7 days, the cell colonies were fixed with 4% paraformaldehyde solution (Beijing Solarbio Biotechnology Co., Ltd.) for 15 min at room temperature. Cells were rinsed three times with PBS and then stained with 0.1% crystal violet solution (Beijing Solarbio Biotechnology Co., Ltd.) according to the manufacturer's instructions. The number of colonies and the number of cells within the colonies were counted in five randomly selected fields under an optical microscope (magnification, x40).

Cell cycle analysis. CRC cells in the logarithmic growth phase were seeded into 6-well plates ($5x10^5$ cells/well), and then incubated with various concentrations of AC (0.1, 0.5 and 2 μM) for 24 and 72 h. The cells were collected, digested with 0.25% trypsin (Gibco; Thermo Fisher Scientific, Inc.) and centrifuged at 200 x g for 4 min at 4˚C. Subsequently, the cells were fixed with 70% pre-cooled ethanol (prepared in PBS) overnight at 4˚C, followed by centrifugation at 700 x g for 4 min at 4˚C. Cells were rinsed with 1 ml pre-cooled PBS and resuspended in pre-cooled PBS at a density of $1x10^6$ cells/ml. Next, 100 μl cell suspension was treated with 10 μg/ml RNase A. Cells were incubated with 20 μg/ml propidium iodide (PI) solution at room temperature for 10 min and then centrifuged at 700 x g for 4 min at 4˚C. The cells were then rinsed with pre-chilled PBS and resuspended in pre-chilled PBS. Flow cytometry was performed to assess the cell cycle using a CytoFLEX flow cytometer (Beckman Coulter, Inc.). Data were analyzed using FlowJo (version 7.6.1; FlowJo LLC).

Cell apoptosis analysis. Cell apoptosis analysis was performed using the Annexin V-Alexa Fluor 488/PI kit (cat. no. CA1040, Beijing Solarbio Biotechnology Co., Ltd.) according to the standard procedures. CRC cells were treated with various concentrations of AC (0.1, 0.5 and 2 μM) for 24 and 72 h. Cells were collected, rinsed twice in PBS and then resuspended in a binding buffer. The cells were subsequently stained with Annexin V-Alexa Fluor 488/PI for 5 min at room temperature following the manufacturer's instructions, and cell apoptosis detected using a CytoFLEX flow cytometer (Beckman Coulter, Inc.). Data analysis was performed using FlowJo (version 7.6.1; FlowJo LLC).

Analysis of mitochondrial membrane potential. Mitochondrial Membrane Potential assay kit with JC-1 (cat. no. M8650; Beijing Solarbio Biotechnology Co., Ltd.) was used to evaluate the mitochondrial membrane potential of CRC cells following treatment with AC. CRC cells in the logarithmic growth phase were seeded into 6-well plates ($5x10^5$ cells/well), and then treated with various concentrations of AC (0.1, 0.5 and 2 μM) for 72 h. The cells were harvested, rinsed twice with PBS and incubated with 1.2 μg/ml phenol red-free medium containing JC-1 probes for 30 min at 37˚C. Subsequently, the cells were collected, rinsed and resuspended in PBS. Fluorescence of the cells was measured using a CytoFLEX flow cytometer (Beckman Coulter, Inc.) at wavelengths of 590 and 530 nm. Data were analyzed using FlowJo (version 7.6.1; FlowJo LLC).

Table I. Primers for reverse transcription-quantitative PCR.

Gene	Forward sequence	Reverse sequence
β-actin	5'-CCTCGCCTTTGCCGATCC-3'	5'-GGATCTTCATGAGGTAGTCAGTC-3'
IκBα	5'-CTCCGAGACTTTCGAGGAAATAC-3'	5'-GCCATTGTAGTTGGTAGCCTTCA-3'
P65	5'-ATGTGGAGATCATTGAGCAGC-3'	5'-CCTGGTCCTGTGTAGCCATT-3'
Caspase-9	5'-CTCAGACCAGAGATTCGCAAAC-3'	5'-GCATTTCCCCTCAAACTCTCAA-3'
Caspase-3	5'-AGAGGGGATCGTTGTAGAAGTC-3'	5'-ACAGTCCAGTTCTGTACCACG-3'
P21	5'-TGTCCGTCAGAACCCATGC-3'	5'-AAAGTCGAAGTTCCATCGCTC-3'
Bax	5'-CCCAGAGTTTGAGCCGAGTG-3'	5'-CCCATCCCTTCGTCGTCCT-3'
Cyclin D1	5'-CAATGACCCCGCACGATTTC-3'	5'-CATGGAGGGCGGATTGGAA-3'
CDK4	5'-CTGGTGTTTGAGCATGTAGACC-3'	5'-GATCCTTGATCGTTTCGGCTG-3'
Bcl-2	5'-CCAGCGTATATCGGAATGTGG-3'	5'-CCATGTGATACCTGCTGAGAAG-3'
P53	5'-GTTTCCGTCTGGGCTTCTTG-3'	5'-CACAACCTCCGTCATGTGCT-3'

Reverse transcription-quantitative polymerase chain reaction (RT-qPCR) analysis. TRIzol reagent (Thermo Fisher Scientific, Inc.) was used to isolate the total RNA from CRC cells treated with AC. The concentration and purity of RNA was detected with a UV spectrophotometer (A260/A280). A ratio of A260/A280 between 1.8 and 2.0 was regarded as a sufficient quality. A quantity of 500 ng total RNA was reverse transcribed into cDNA using a PrimeScript™ RT Master mix (cat. no. RR036A; Takara Bio, Inc.). The RT conditions were 37˚C for 15 min, followed by 85˚C for 5 sec, and storage at 4˚C. qPCR was performed on a LightCycler® 96 system (Roche Diagnostics) using One Step TB Green® PrimeScript™ RT-PCR kit (cat. no. RR066A; Takara Bio, Inc.). The thermocycling conditions were as follows: Pre-denaturation at 95˚C for 2 min; 40 cycles of denaturation at 95˚C for 30 sec, annealing at 60˚C for 30 sec, and extension at 72˚C for 30 sec. The relative expression levels of genes were calculated using the $2^{-\Delta\Delta Cq}$ method (21), and β-actin was used as an internal control. The experiment was performed in triplicate. All primer sequences used in the present study are listed in Table I.

Western blotting. Total protein was extracted from CRC cells or tumor tissues using RIPA lysis buffer (Beyotime Institute of Biotechnology) containing 1% protease inhibitor (Beyotime Institute of Biotechnology). Protein concentration was determined using a BCA protein assay kit (Nanjing KeyGEN Biotech, Co., Ltd.) according to the manufacturer's protocol. Subsequently, proteins (30 μg per lane) were separated by 10% SDS-PAGE (Nanjing KeyGEN Biotech, Co., Ltd.) and then transferred onto polyvinylidene fluoride membranes (EMD Millipore). The membranes were blocked with 5% skimmed milk (prepared in TBST containing 0.1% Tween-20) for 2 h at room temperature and incubated with corresponding primary antibodies overnight at 4˚C. The following primary antibodies were used for incubation: Anti-NF-kB P65 (1:1,000; cat. no. ab16502; Abcam), anti-phosphorylated (p)-P65 (1:1,500; cat. no. ab86299; Abcam), anti-caspase-3 (1:1,000; cat. no. ab4051, Abcam), anti-cleaved caspase-3 (1:1,000; cat. no. ab32042; Abcam), anti-caspase-9 (1:1,000; cat. no. ab32539; Abcam), anti-cleaved caspase-9 (1:1,000; cat. no. ab32539; Abcam), anti-Bcl-2 (1:1,000; cat. no. ab32124; Abcam), anti-Bax (1:1,000; cat. no. ab32503; Abcam), anti-CDK4 (1:1,000; cat. no. ab199728, Abcam), anti-Cyclin D1 (1:2,000; cat. no. ab205718; Abcam), anti-IκBα (1:1,000; cat. no. 9242; Cell Signaling Technology, Inc.), anti-p-IκBα (1:1,000; cat. no. 2859; Cell Signaling Technology, Inc.), anti-Histone H3 (1:3,000; cat. no. ab1791; Abcam) and anti-β-actin (1:5,000; cat. no. ab8227; Abcam). Subsequently, the membranes were incubated with horseradish peroxidase (HRP)-conjugated goat anti-rabbit IgG H&L (1:5,000; cat. no. ab205718; Abcam) or HRP-conjugated goat anti-mouse IgG H&L (1:5,000; cat. no. ab205719; Abcam) secondary antibodies for 2 h at room temperature. The immunoreactive proteins were then visualized using immobilon western chemiluminescent HRP substrate (EMD Millipore). The western blots were analyzed with Image Lab 3.0 software (Bio-Rad Laboratories, Inc.).

Nuclear/cytosol fractionation kit assay. Nuclear and cytosolic fractions were prepared using the nuclear/cytosol extraction kit (cat. no. K266-25; BioVision, Inc.) according to the manufacturer's instructions. All buffers were stored in ice throughout the experimental period. All centrifugation steps were performed at 4˚C. CRC cells were treated with AC (2 μM) for 72 h at 37˚C, harvested and rinsed twice with pre-cooled PBS. Cells were subsequently centrifuged at 600 x g for 5 min. A total of $1x10^6$ cells were treated with 200 μl pre-chilled CEB-A mix (1 ml CEB-A mix containing 1 μl DTT and 2 μl protease inhibitor), vortexed vigorously for 15 sec to fully resuspend the cell pellets and incubated on ice for 10 min. Subsequently, 11 μl pre-cooled cytosol extraction buffer-B was added, vortexed vigorously for 5 sec, and incubated on ice for 1 min. The tube was continuously vortexed vigorously for 5 sec, followed by centrifugation at 14,000 x g for 5 min. The supernatant (cytoplasmic extract) was immediately transferred to a clean pre-cooled tube and the tube was placed on ice.

Next, 100 μl ice-cold nuclear extraction buffer mix (1 ml NEB containing 2 μl protease inhibitor cocktail and 1 μl DTT) was added to the cell pellets (nuclei), and then vortexed vigorously for 10 sec. The cell pellets were placed on ice for 40 min, vortexed for 15 sec and the samples placed on ice after 10 min. Finally, following centrifugation at 16,000 x g for 5 min, the supernatant (nuclear extract) was immediately transferred into

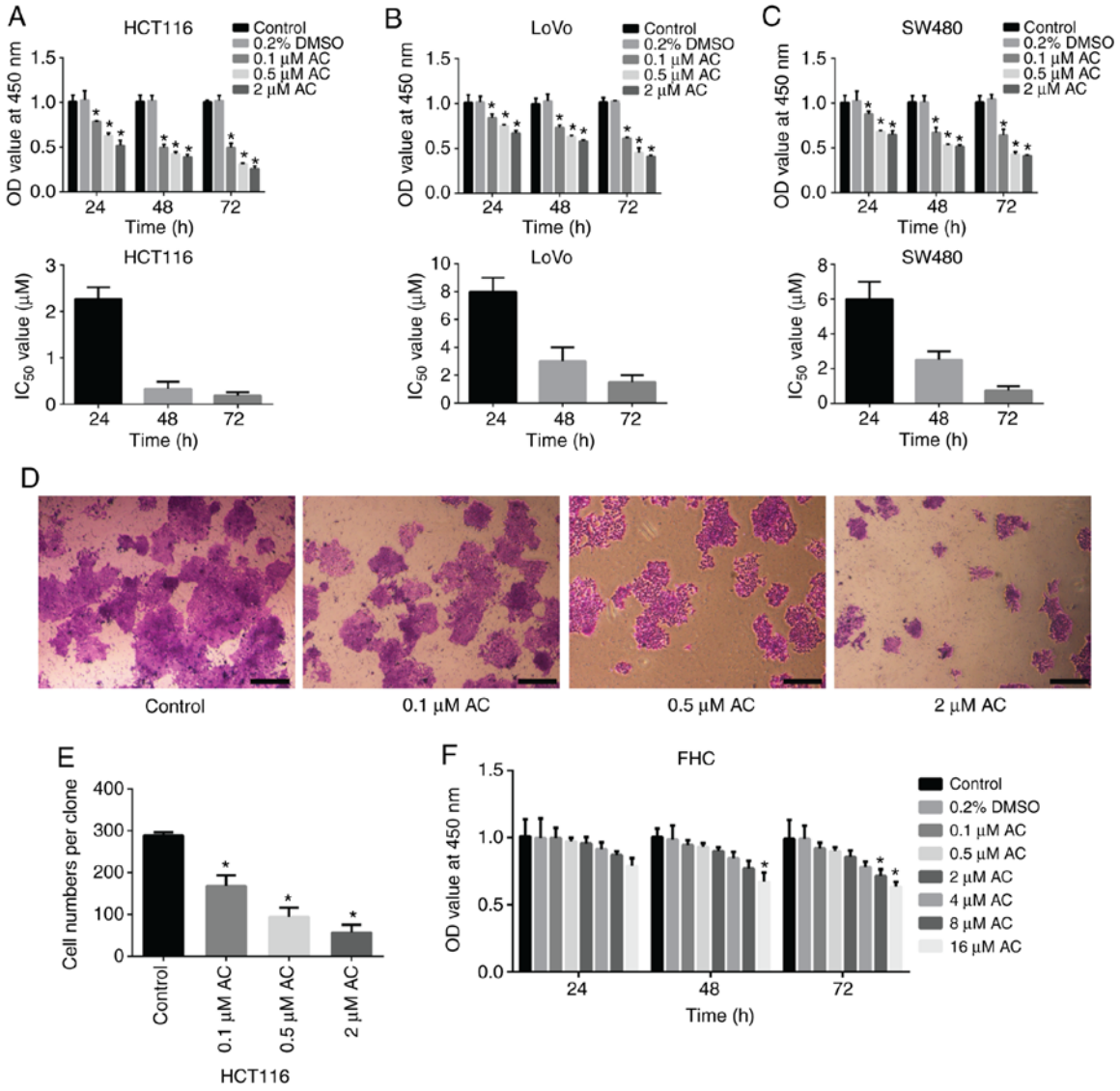

Figure 1. Effect of AC on the viability and colony formation of colorectal cancer cells. AC inhibited the viability of (A) HCT116, (B) LoVo and (C) SW480 cells in a time and dose-dependent manner. The corresponding IC_{50} values were measured. (D) The effects of different concentrations of AC on colony formation in HCT116 cells. Magnification, x40. Scale bar, 200 μm. (E) Quantitative analysis of cell numbers per clone. (F) Effect of asiaticoside on the viability of normal human intestinal FHC cells. Data are expressed as mean ± standard deviation from three independent experiments. $^{*}P<0.05$ vs. control cells. AC, asiaticoside; IC_{50}, the half maximal inhibitory concentration; OD, optical density.

a pre-cooled clean tube and stored at -80˚C. The cytosol and nuclear extracts were then used for western blotting to measure P65 expression level.

Animal experiments. A total of 18 5-week-old female BALB/c-nude mice (weight, 20-25 g) were purchased from the Model Animal Research Center of Nanjing University and maintained according to regulations of the Animal Care Committee of The First Affiliated Hospital of Xiamen University. The housing conditions of mice were as follows: The temperature was 22-24˚C, humidity was 45-60%, ventilation was 15 times/h, and 12 h of light and 12 h of dark. Mice were provided food and water *ad libitum*. In the present study, mice were randomly divided into three groups (n=6 per group): i) Control group; ii) 5 mg/kg AC treatment group; and iii) 10 mg/kg AC treatment group. HCT116 cells ($5x10^6$) were subcutaneously injected into the right hind legs of the mice. Subsequently, 1 week later, 5 or 10 mg/kg AC or PBS (10 mg/kg) was administered to mice by oral gavage every 2 days for 6 consecutive weeks. Tumor diameters were measured using calipers every week. Mice were euthanized at 42 days after the first administration of AC or PBS by cervical dislocation, and the tumors were carefully excised and weighed. All mice were in good health throughout the experimental period. All *in vivo* experiments were performed at the Animal Center of The First Affiliated Hospital of Xiamen University (Xiamen, China) according to the guidelines of the National Institutes of Health and approved by the Animal Care and Use Committee of The First Affiliated Hospital of Xiamen University (approval no. XMU-AEA-20180137).

Statistical analysis. Statistical analyses were performed using GraphPad Prism 6.0 software (GraphPad Software, Inc.) and SPSS software version 21.0 (IBM Corp.). Comparisons between groups were performed using one-way analysis of variance with Bonferroni's post hoc analysis. Data from three

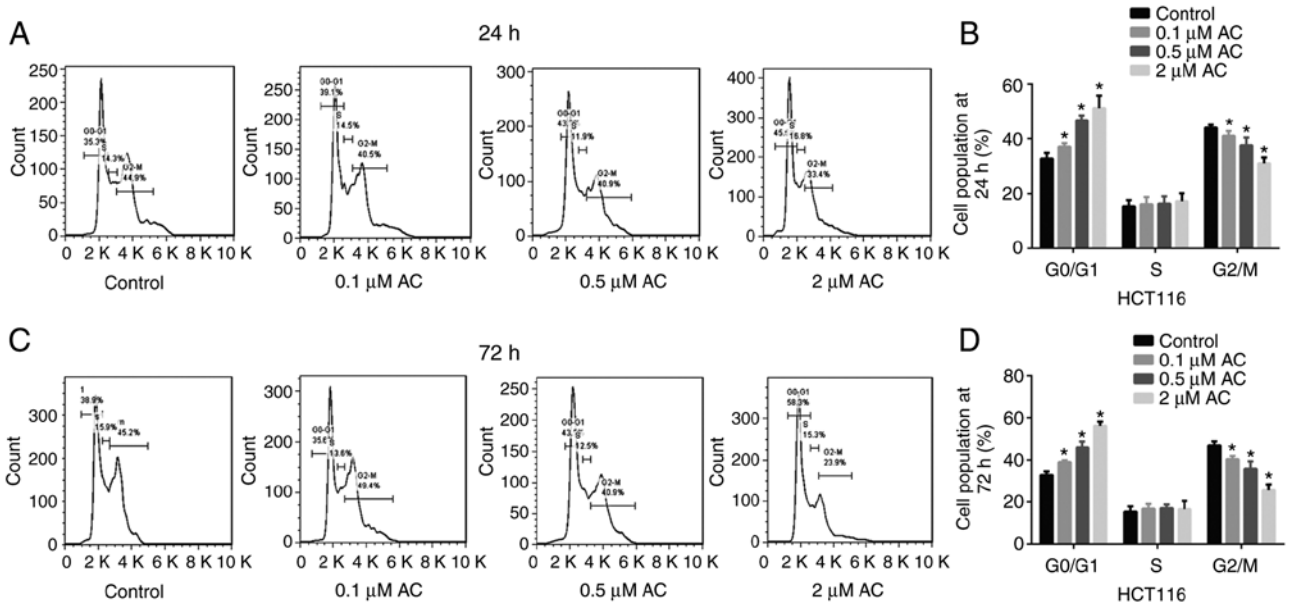

Figure 2. Effect of AC on the cell cycle of colorectal cancer cells. (A) Flow cytometry was used to detect cell cycle distribution in HCT116 cells treated with various concentrations of AC for 24 h and (B) the results were quantified. (C) Flow cytometry was used to detect cell cycle distribution in HCT116 cells treated with various concentrations of AC for 72 h and (D) the results were quantified Data are expressed as mean ± standard deviation from three independent experiments. *P<0.05 vs. control cells. AC, asiaticoside.

independent experiments are expressed as the mean ± standard deviation. P<0.05 was considered to indicate a statistically significant difference.

Results

AC inhibits CRC cell proliferation and induces CRC cell cycle arrest at the G0/G1 phase. CCK-8 assay and colony formation assay were performed to determine the effect of AC on the viability of CRC cells. Results of the CCK-8 assay demonstrated that AC significantly reduced the viability of HCT116, SW480, and LoVo cells in a time and dose-dependent manner (Fig. 1A-C), whereas AC had no significant effects on normal human intestinal FHC cells at a given range of concentrations (0.1-8 μM) (Fig. 1F). However, the viability of FHC cells was significantly reduced after treating with 16 μM AC for 72 h, indicating that high concentration of AC has an adverse effect on human normal epithelial cells. Additionally, HCT116 cells, with the lowest IC_{50} value, were selected for subsequent analyses. Colony formation assay revealed that AC significantly inhibited the colony formation of HCT116 cells in a dose-dependent manner (Fig. 1D and E). Furthermore, flow cytometry analysis indicated that AC treatment for 24 or 72 h significantly induced CRC cell cycle arrest at the G0/G1 phase. The percentage of cells in the G2/M phase significantly decreased following treatment with AC for 24 or 72 h and no difference was observed for the percentage of cells in the S phase (Fig. 2).

AC suppresses the expression levels of cell cycle-associated genes. RT-qPCR and western blotting assays were performed to further understand the specific mechanism of the effects of AC on the CRC cell cycle. The findings revealed that AC significantly decreased the expression levels of CDK4 and Cyclin D1, whereas the expression levels of P53 and P21 were significantly higher in AC-treated cells compared with the control cells (Fig. 3).

AC decreases mitochondrial membrane potential and promotes CRC cell apoptosis. In the present study, JC-1 probes were used to measure mitochondrial membrane potential, and cell apoptosis was detected using flow cytometry. JC-1, a cyanine dye, promotes discrimination of energized and deenergized mitochondria, where the normally green fluorescent dye forms red fluorescent aggregates when concentrated in energized mitochondria (22). However, when cell apoptosis occurs, the mitochondrial transmembrane potential is decreased, JC-1 is released from the mitochondria, decreasing in concentration and maintaining the monomeric form with green fluorescence. Therefore, it is widely used to determine the apoptosis of the cell by detecting green (low) and red (high) fluorescence. The present results indicated that AC significantly decreased the mitochondrial membrane potential of HCT116 cells in a dose-dependent manner (Fig. 4A and B). Furthermore, AC significantly increased the apoptosis of CRC cells compared with the untreated cells (Fig. 4C-F).

AC regulates the expression of apoptosis-related genes in CRC cells. RT-qPCR and western blotting were performed to further elucidate the biological function of AC in CRC cells (Fig. 5). The results demonstrated that AC significantly increased the activation of caspase-9 and caspase-3 in HCT116 cells in a dose-dependent manner (Fig. 5C), but had no effect on the mRNA levels of caspase-9 and caspase-3 (Fig. 5A). In addition, AC significantly downregulated Bcl-2 expression and upregulated Bax expression at both the mRNA and protein levels (Fig. 5A-C. The ratio of Bcl-2/Bax protein expression was significantly decreased following AC treatment compared with the control cells (Fig. 5C).

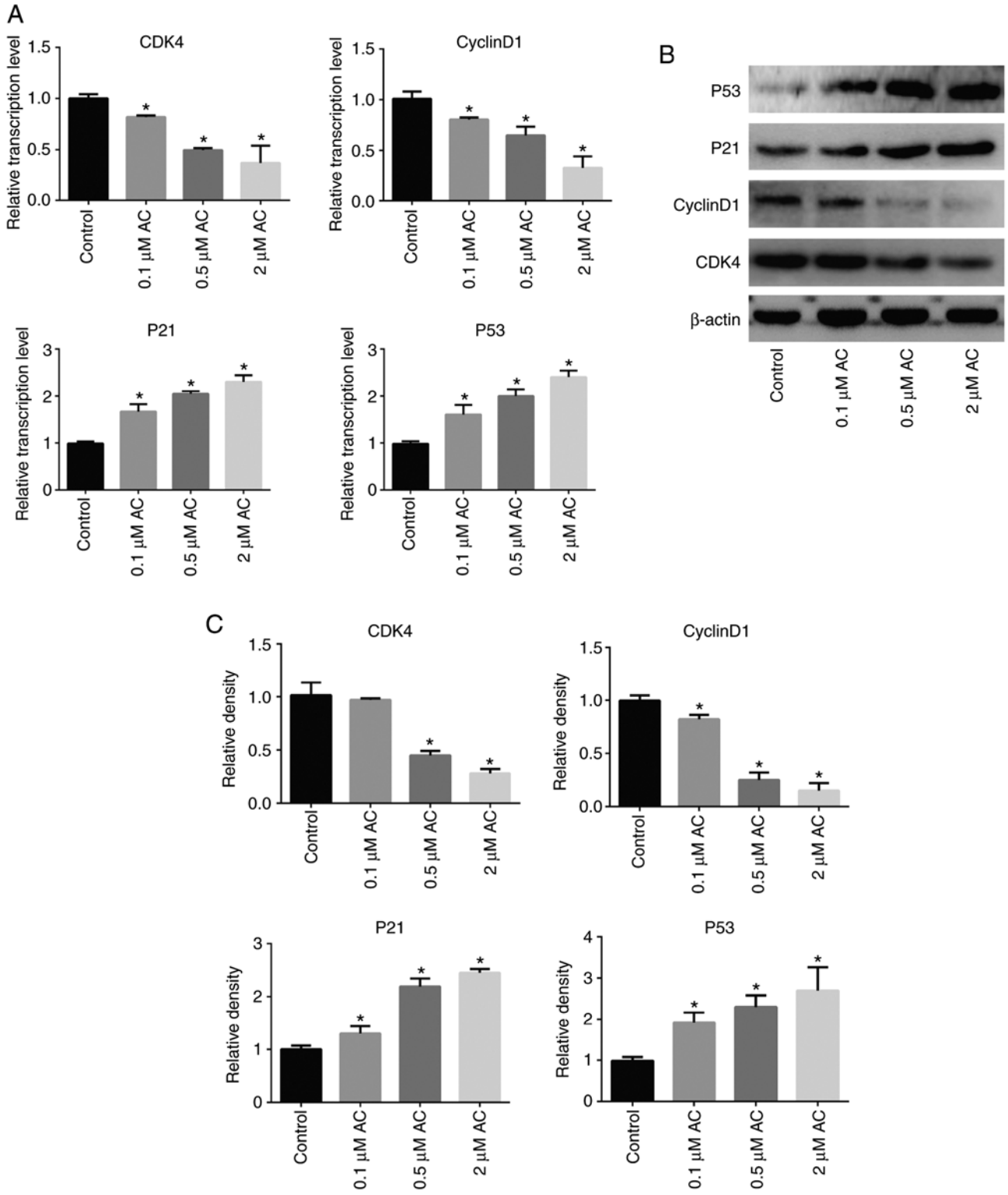

Figure 3. Effect of AC on the expression of genes associated with the cell cycle. (A) mRNA levels of CDK4, Cyclin D1, P53 and P21 in HCT116 cells treated with AC for 72 h. (B) Representative western blots of CDK4, Cyclin D1, P53 and P21 in HCT116 cells treated with AC for 72 h; and (C) quantification. Data are expressed as mean ± standard deviation from three independent experiments. *P<0.05 vs. control cells. AC, asiaticoside.

AC suppresses phosphorylation of IκBα and NF-κB p65, inhibiting the NF-κB signaling pathway. The NF-κB signaling pathway is crucial for the regulation of various biological activities of eukaryotic cells, such as cell proliferation, survival and apoptosis (23,24). Inhibitors of the NF-κB signaling pathway are potential anticancer drug candidates (25). The present study assessed the activation and expression of molecules associated with the NF-κB pathway in HCT116 cells treated with AC using RT-qPCR and western blotting (Fig. 6). The results revealed that treatment of HCT116 cells with AC significantly decreased phosphorylation of IκBα and P65 (Fig. 6B and C), but had no effect on the mRNA levels of

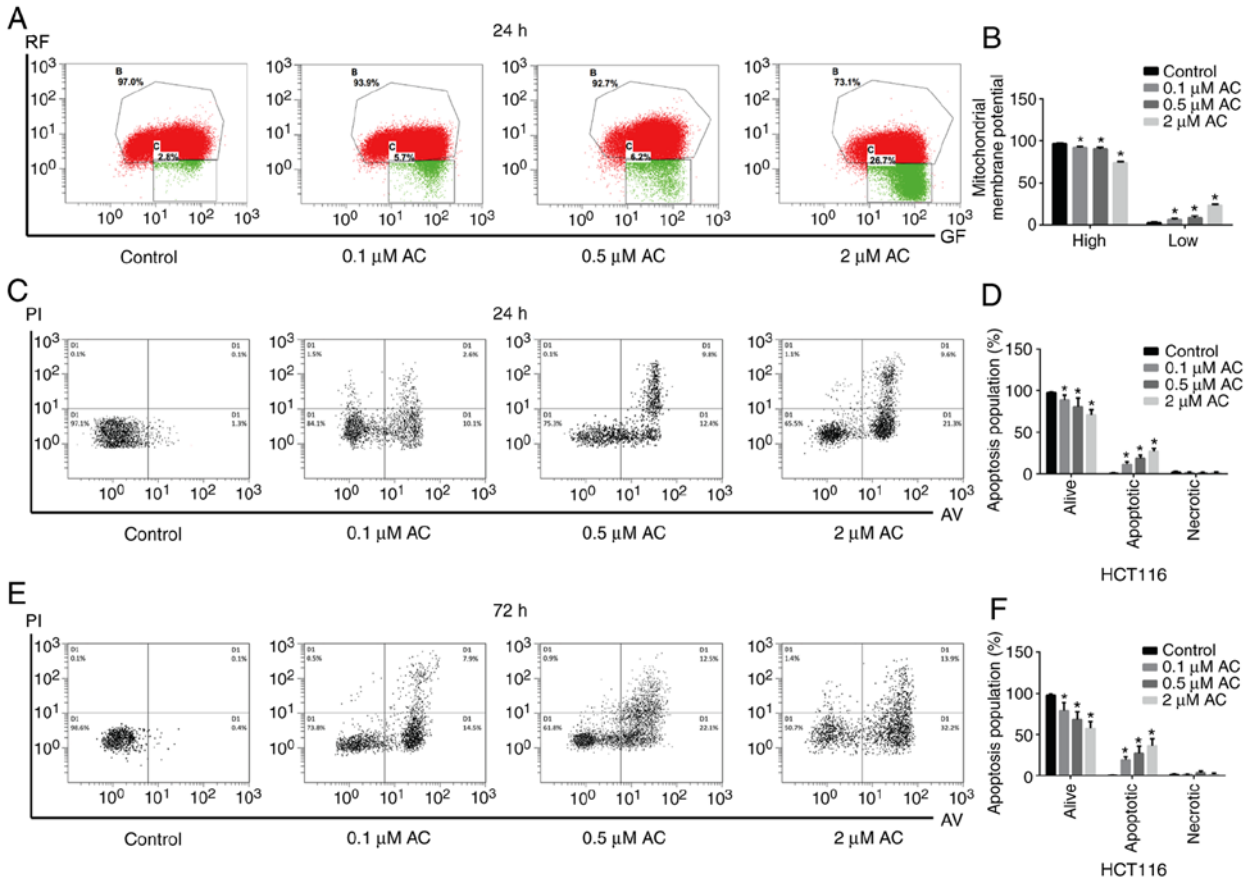

Figure 4. Effect of Ac on mitochondrial membrane potential and colorectal cancer cell apoptosis. (A) AC treatment for 24 h decreased mitochondrial membrane potential in HCT116 cells, where the apoptosis of CRC cells was determined by detecting the intensity of green (low) fluorescence from red (high) fluorescence. (B) Quantification of the mitochondrial membrane potential. (C) The apoptosis of HCT116 cells treated with various concentrations of AC for 24 h was measured by flow cytometry and (D) statistically analyzed. (E) The apoptosis of HCT116 cells treated with various concentrations of AC for 72 h was detected by flow cytometry and (F) statistically analyzed. Data are expressed as mean ± standard deviation from three independent experiments. *P<0.05 vs. control cells. AC, asiaticoside; RF, red fluorescence; GF, green fluorescence; PI, propidium iodide; AV, Annexin-V.

total IκBα and P65 compared with the control cells (Fig. 6A). Furthermore, AC significantly increased the content of P65 in the nucleus, but decreased P65 content in the cytoplasm, suggesting that AC treatment inhibited nuclear translocation of P65 (Fig. 6D and E).

Synergistic inhibitory effects of AC and the NF-κB signaling pathway inhibitor JSH-23 on CRC cells. Administration of 0.5 μM AC and the NF-κB signaling pathway inhibitor JSH-23 (100 nM) significantly suppressed CRC cell viability, significantly induced cell cycle arrest at the G0/G1 phase, significantly promoted cell apoptosis and significantly deceased the phosphorylation of IκBα and P65 in HCT116 cells in comparison to HCT 116 cells treated either with AC or JSH-23 (Fig. 7). A synergistic inhibitory effect of AC and JSH-23 on CRC cells was observed, indicating that AC may be a promising adjuvant agent in treatment of CRC.

AC inhibits CRC tumor cell growth in vivo. The present findings revealed that administration of AC in mice with tumors notably inhibited tumor growth; tumor diameters and tumor volumes were significantly decreased in comparison with the control group (Fig. 8A and B). Furthermore, RT-qPCR and western blotting revealed that the protein expression levels of P53, P21 and Bax were significantly upregulated, whereas expression levels of CDK4, Cyclin D1 and Bcl-2 were significantly downregulated in tumor tissues following treatment with AC compared with untreated controls. Moreover, administration of AC caused a significant decrease in the phosphorylation of IκBα and P65 (Fig. 8C and D). These results were consistent with those of the *in vitro* analysis.

Discussion

The present study revealed that AC, a plant-derived triterpenoid, induced cell cycle arrest at the G0/G1 phase, promoted CRC cell apoptosis and suppressed cell viability. AC treatment contributed to the aberrant expression of the cell cycle-related genes CDK4, Cyclin D1 and P53 and P21. AC increased the activation of caspase-9 and caspase-3 (apoptosis-related genes), upregulated Bax level, and downregulated Bcl-2 expression. Furthermore, AC inhibited the phosphorylation of IκBα and NF-κB p65, resulting in the inhibition of the NF-κB signaling pathway. This consequently affects various biological activities in eukaryotic cells, including cell proliferation, survival and apoptosis. Furthermore, a synergistic inhibitory effect of AC and the NF-κB signaling pathway inhibitor, JSH-23 on CRC was observed. AC suppressed proliferation of CRC cells

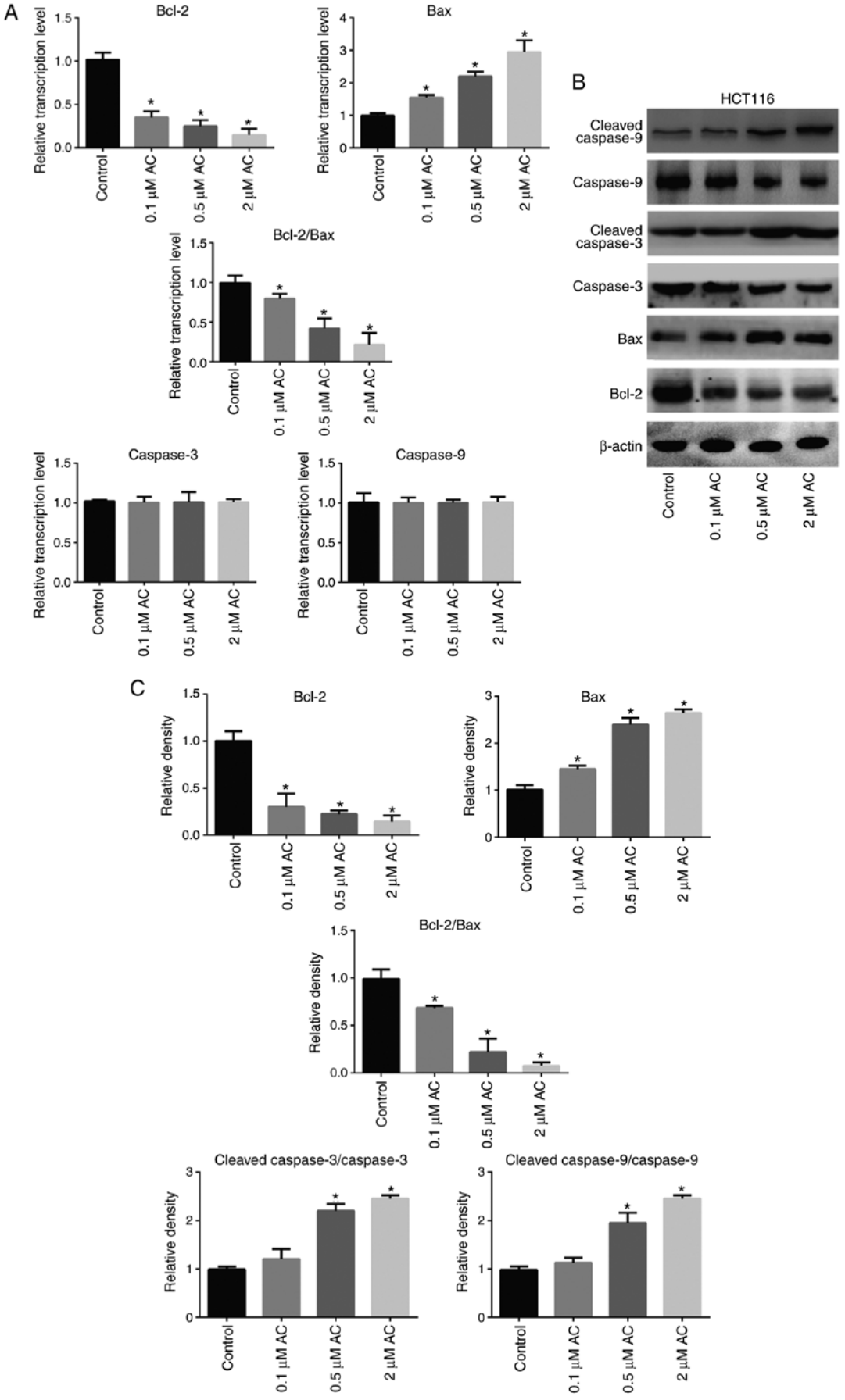

Figure 5. Effect of Ac on the expression of apoptosis-related genes in colorectal cancer cells. (A) The mRNA levels of Bax, Bcl-2, caspase-3 and caspase-9 in HCT116 cells treated with AC for 72 h. (B) Protein levels of Bax, Bcl-2, caspase-3, cleaved caspase-3, caspase-9 and cleaved caspase-9 in HCT116 cells treated with AC for 72 h. (C) Quantification of the western blots. Data are expressed as mean ± standard deviation from three independent experiments. *P<0.05 vs. control cells. AC, asiaticoside.

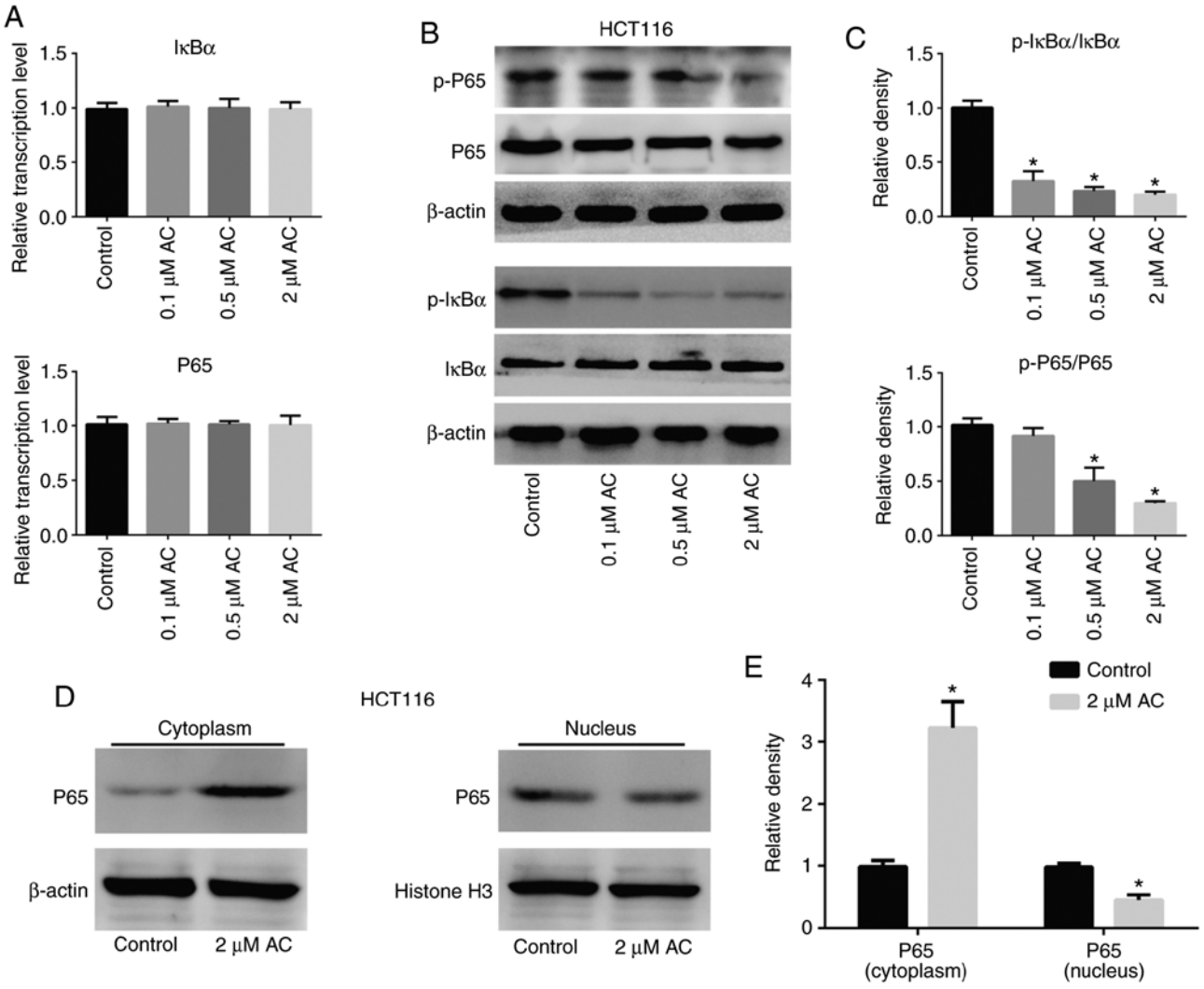

Figure 6. Effect of AC on the NF-κB signaling pathway. (A) mRNA and (B) protein expression levels of the NF-κB signaling pathway-related molecules IκBα, p-IκBα, P65 and p-P65 in HCT116 cells treated with AC for 72 h. (C) Quantification of the western blots. (D) Nuclear translocation of P65 detected by western blotting in HCT116 cells treated with 2 μM AC for 72 h. (E) Quantification of the western blots. Data are expressed as mean ± standard deviation from three independent experiments. *P<0.05 vs. control cells. AC, asiaticoside; p-, phosphorylated.

both *in vitro* and *in vivo*, implying that it can be a potential adjuvant agent for the treatment of CRC.

A number of studies have demonstrated that AC exhibits antitumor activity (17,18,20). AC increases the sensitivity of the human oral epithelial cancer cells and breast cancer cells to chemotherapy drugs by increasing intracellular reactive oxygen species and activating apoptotic pathways *in vitro* (19). AC inhibits breast cancer progression in mice by downregulating IL-1β expression and activating downstream signaling pathways *in vivo* (20). The present study demonstrated that AC significantly suppressed proliferation and colony formation in CRC cells. Decreased mitochondrial membrane potential is a common phenomenon of mitochondrial apoptosis in cancer cells (4), which results in the release of mitochondrial apoptogens to initiate the caspase cascade, causing programmed cell death (26,27). The present study identified that AC treatment for 24 h decreased the mitochondrial membrane potential in HCT116 cells and induced CRC cell apoptosis. At this point, the proportion of cell apoptosis in the AC-treated group was not so high, but the mitochondrial membrane potential was significantly altered, indicating that the change of mitochondrial membrane potential occurred earlier than cell apoptosis. When HCT116 cells were treated with AC for 72 h, cell apoptosis was significantly elevated in comparison with the untreated cells. Hence, the mitochondrial membrane potential was not detected.

Previous studies have demonstrated that the decreased ratio of Bcl-2/Bax regulates apoptosis in cells (28,29). In the present study, AC-induced cell apoptosis was coupled with upregulation of Bax, cleaved caspase-3 and cleaved caspase-9, and the downregulation of Bcl-2. Additionally, the cell cycle transition from G0/G1 to S is effected by multiple genes, such as CDK4/6 and Cyclin D1 (30). A study has indicated that downregulation of CDK4 expression causes cell cycle arrest at the G0/G1 phase (31), which may explain the mechanism of antitumor effects of several drugs. The present results indicated that AC significantly inhibited the proliferation of CRC cells by interrupting the cell cycle at the G0/G1 phase. AC treatment substantially reduced the expression of CDK4 and Cyclin D1. However, the specific mechanism involved in the regulation of CDK4 and Cyclin D1 gene expression remains unknown.

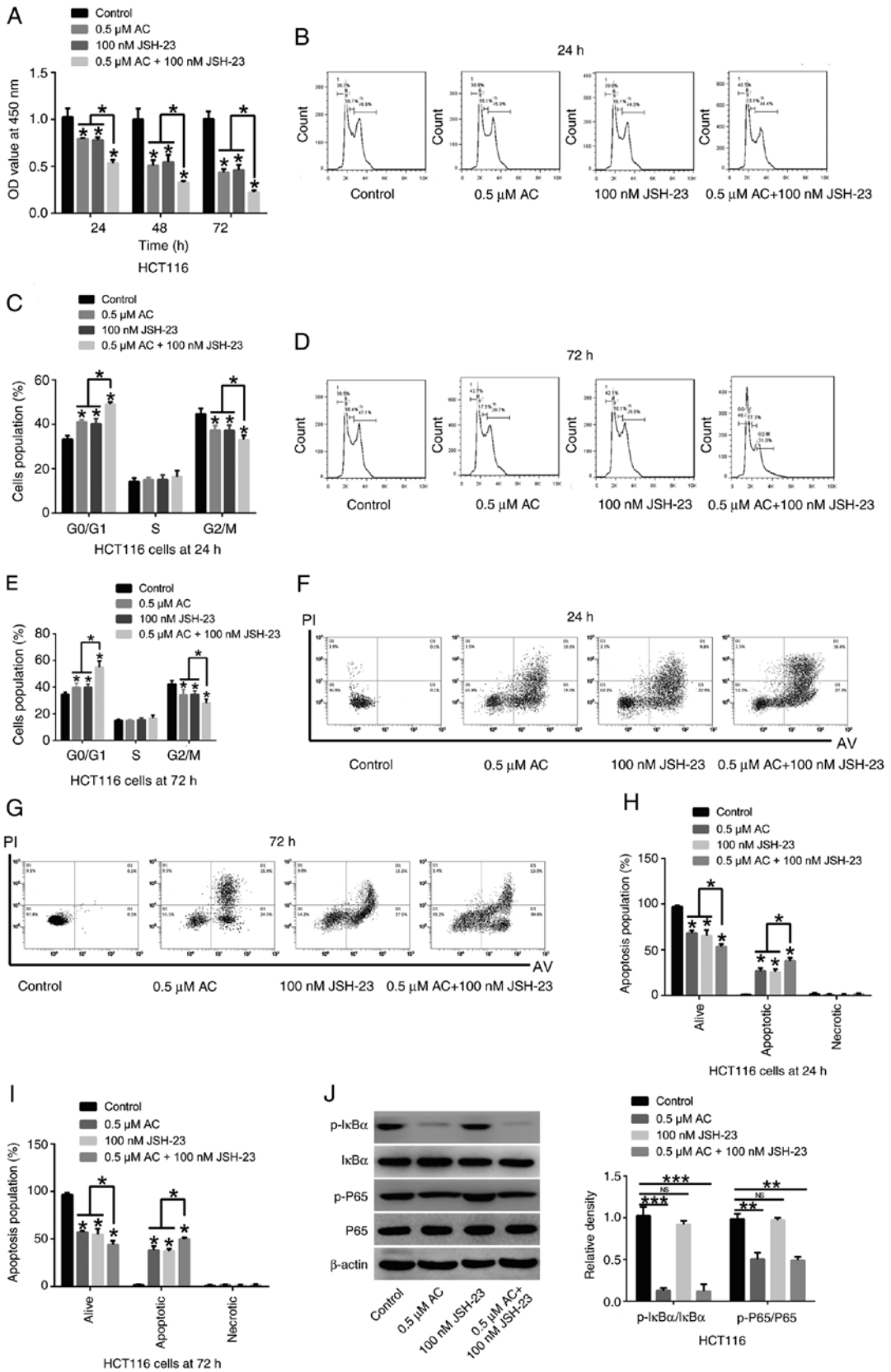

Figure 7. Synergistic inhibitory effects of AC and the NF-κB signaling pathway inhibitor JSH-23 on colorectal cancer cells. (A) CCK-8 assay was performed to detect the viability of HCT116 cells treated with AC and JSH-23 for 24, 48 and 72 h. (B) Cell cycle of HCT116 cells treated with AC and JSH-23 for 24 h was assessed using flow cytometry. (C) Statistical analysis of cell cycle of HCT116 cells co-treated with AC and JSH-23 for 24 h. (D) Cell cycle of HCT116 cells co-treated with AC and JSH-23 for 72 h was measured by flow cytometry. (E) Quantification of cell cycle of HCT116 cells co-treated with AC and JSH-23 for 72 h. (F) Cell apoptosis of HCT116 cells co-treated with AC and JSH-23 for 24 h was determined using flow cytometry. (G) Cell apoptosis of HCT116 cells co-treated with AC and JSH-23 for 72 h was detected by flow cytometry. (H) Statistical analysis of cell apoptosis of HCT116 cells co-treated with AC and JSH-23 for 24 h. (I) Statistical analysis of cell apoptosis of HCT116 cells co-treated with AC and JSH-23 for 72 h. (J) The phosphorylation of IκBα and P65 was measured by western blotting. Data are expressed as mean ± standard deviation from three independent experiments. *P<0.05, **P<0.01, ***P<0.001 vs. control cells or as indicated. AC, asiaticoside; p-, phosphorylated; OD, optical density; NS, not significant.

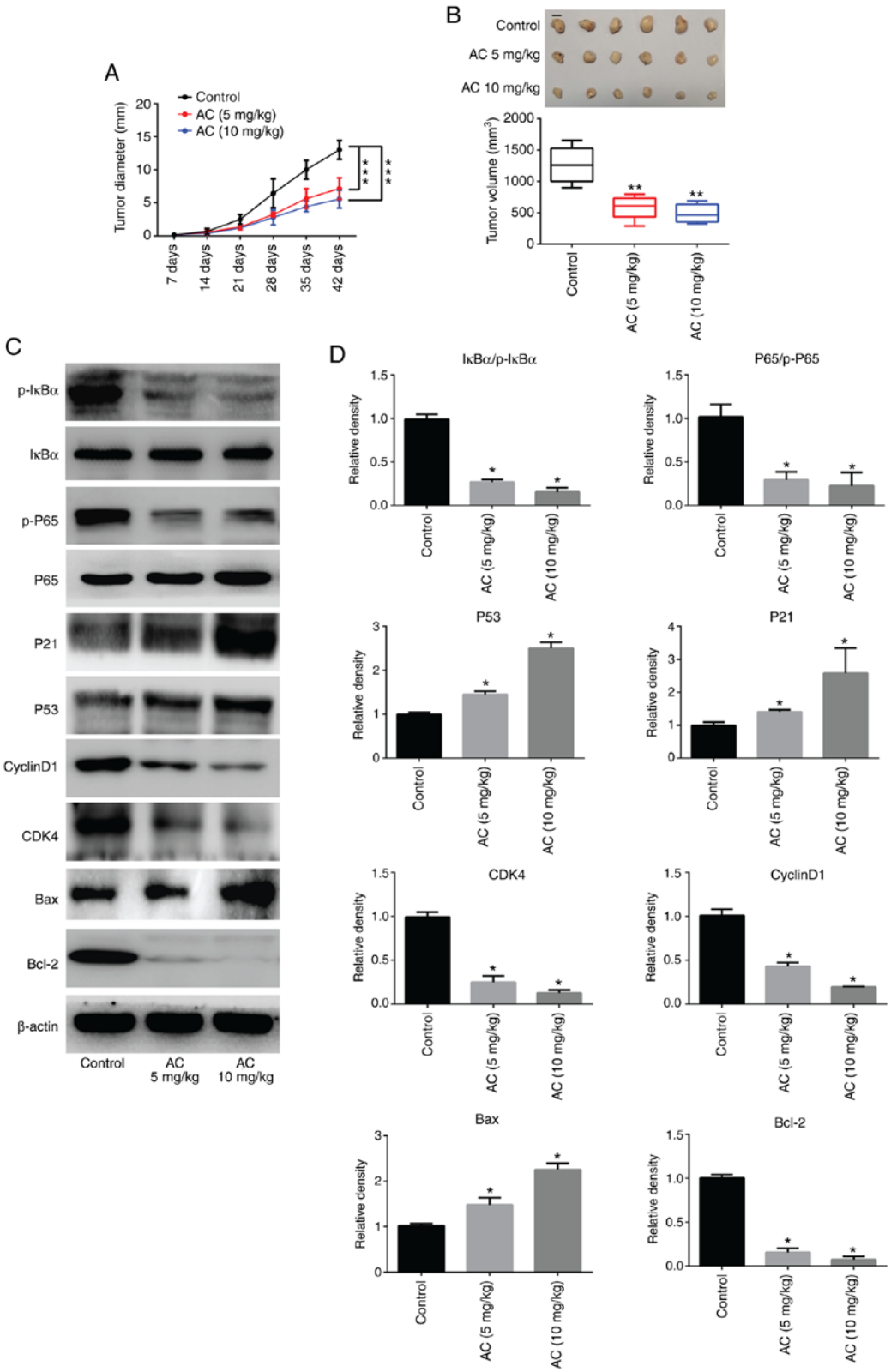

Figure 8. AC inhibits colorectal cancer growth in a nude mouse model. (A) Measurement of tumor diameters using a caliper in xenografted nude mice treated with AC (n=6 mice per group). (B) Representative images of tumor sizes at 42 days and measurement of tumor volume at 42 days after excision (n=6 mice per group). (C) The protein levels of P53, P21, CDK4, Cyclin D1, Bax, and Bcl-2 in excised tumor tissues. (D) Western blotting was performed three times independently and quantified. Data are expressed as mean ± standard deviation. *P<0.05, **P<0.01, ***P<0.001 vs. control group. AC, asiaticoside; p-, phosphorylated.

AC suppresses the inflammatory response after injury via regulation of the NF-κB signaling pathway (14,32,33). IκBα is an inhibitory protein of the NF-κB signaling pathway that normally binds to P65 resulting in the inhibition of P65 phosphorylation and its nuclear translocation (34). Conversely, IκBα phosphorylation promotes its own ubiquitination and degradation, thereby eliminating the inhibitory effect on P65 (35,36). Once P65 enters the nucleus, it triggers a series of

gene expressions such as Bcl-2 and CDK4 (37). Results of the present study revealed that AC treatment significantly reduced IκBα and P65 phosphorylation, resulting in inhibition of P65 nuclear translocation and interfering with the expression of downstream molecules. Although results of the *in vivo* experiments demonstrated that AC administration significantly inhibited tumor growth without evident adverse effects on mice, the clinical use of AC as an antitumor drug requires further study.

In conclusion, AC inhibited activation of the NF-κB signaling pathway and subsequently modulated the expression of its downstream genes by attenuating IκBα and P65 phosphorylation, which may induce apoptosis and cell cycle arrest in CRC cells. Thus, proliferation of CRC cells *in vitro* and tumor growth *in vivo* were suppressed. Therefore, AC is a promising adjuvant with antitumor effects in CRC.

Acknowledgements

Not applicable.

Funding

This study was financed by the National Social Science Foundation of China (grant no. 81871877), National Major Scientific and Technological Special Project for 'Significant New Drugs Development' (grant no. 2020ZX09201005) and Youth Foundation of Xiamen Cancer Center (grant nos. ZLYYA201710 and ZLYYA201704).

Availability of data and materials

The datasets used and/or analyzed during the current study are available from the corresponding author on reasonable request.

Authors' contributions

YM and CK conceived and designed the study. XZ, YL and YM analyzed the experimental data. YM and CK acquired the funding. XZ, YL, CR, TL and FD performed the experiments. XZ, YL, CR, YM and CK participated in the design of the experimental methods. XZ, YM and CK wrote the manuscript. All authors read and approved the final manuscript.

Ethics approval and consent to participate

All animal experiments were approved by the Animal Care and Use Committee of The First Affiliated Hospital of Xiamen University (Xiamen, China; approval no. XMU-AEA-20180137) and carried out in accordance with the Guide for the Care and Use of Laboratory Animals.

Patient consent for publication

Not applicable.

Competing interests

The authors declare that there have no competing interests.

References

1. Siegel RL, Miller KD and Jemal A: Cancer statistics, 2019. CA Cancer J Clin 69: 7-34, 2019.
2. Miller KD, Nogueira L, Mariotto AB, Rowland JH, Yabroff KR, Alfano CM, Jemal A, Kramer JL and Siegel RL: Cancer treatment and survivorship statistics, 2019. CA Cancer J Clin 69: 363-385, 2019.
3. Van der Jeught K, Xu HC, Li YJ, Lu XB and Ji G: Drug resistance and new therapies in colorectal cancer. World J Gastroenterol 24: 3834-3848, 2018.
4. Bahrami A, Amerizadeh F, Hassanian SM, ShahidSales S, Khazaei M, Maftouh M, Ghayour-Mobarhan M, Ferns GA and Avan A: Genetic variants as potential predictive biomarkers in advanced colorectal cancer patients treated with oxaliplatin-based chemotherapy. J Cell Physiol 233: 2193-2201, 2018.
5. Bylka W, Znajdek-Awiżeń P, Studzińska-Sroka E, Dańczak-Pazdrowska A and Brzezińska M: *Centella asiatica* in dermatology: An overview. Phytother Res 28: 1117-1124, 2014.
6. Chandrika UG and Prasad Kumarab Peramune AAS: Gotu Kola (*Centella asiatica*): Nutritional properties and plausible health benefits. Adv Food Nutr Res 76: 125-157, 2015.
7. da Rocha PBR, Santos Souza BD, Andrade LM, Marreto RN, Lima EM and Taveira SF: Development of a high-performance liquid chromatographic method for asiaticoside quantification in different skin layers after topical application of a *Centella asiatica* extract. Planta Med 83: 1431-1437, 2017.
8. Nowwarote N, Osathanon T, Jitjaturunt P, Manopattanasoontorn S and Pavasant P: Asiaticoside induces type I collagen synthesis and osteogenic differentiation in human periodontal ligament cells. Phytother Res 27: 457-462, 2013.
9. Lee J, Jung E, Kim Y, Park J, Park J, Hong S, Kim J, Hyun C, Kim YS and Park D: Asiaticoside induces human collagen I synthesis through TGFbeta receptor I kinase (TbetaRI kinase)-independent Smad signaling. Planta Med 72: 324-328, 2006.
10. Phaechamud T, Yodkhum K, Charoenteeraboon J and Tabata Y: Chitosan-aluminum monostearate composite sponge dressing containing asiaticoside for wound healing and angiogenesis promotion in chronic wound. Mater Sci Eng C Mater Biol Appl 50: 210-225, 2015.
11. Huang J, Zhou X, Shen Y, Li H, Zhou G, Zhang W, Zhang Y and Liu W: Asiaticoside loading into polylactic-co-glycolic acid electrospun nanofibers attenuates host inflammatory response and promotes M2 macrophage polarization. J Biomed Mater Res A 108: 69-80, 2020.
12. Zhang CZ, Niu J, Chong YS, Huang YF, Chu Y, Xie SY, Jiang ZH and Peng LH: Porous microspheres as promising vehicles for the topical delivery of poorly soluble asiaticoside accelerate wound healing and inhibit scar formation in vitro & in vivo. Eur J Pharm Biopharm 109: 1-13, 2016.
13. Qi SH, Xie JL, Pan S, Xu YB, Li TZ, Tang JM, Liu XS, Shu B and Liu P: Effects of asiaticoside on the expression of Smad protein by normal skin fibroblasts and hypertrophic scar fibroblasts. Clin Exp Dermatol 33: 171-175, 2008.
14. Qiu J, Yu L, Zhang X, Wu Q, Wang D, Wang X, Xia C and Feng H: Asiaticoside attenuates lipopolysaccharide-induced acute lung injury via down-regulation of NF-kB signaling pathway. Int Immunopharmacol 26: 181-187, 2015.
15. Luo Y, Fu C, Wang Z, Zhang Z, Wang H and Liu Y: Asiaticoside attenuates the effects of spinal cord injury through antioxidant and antiinflammatory effects, and inhibition of the p38MAPK mechanism. Mol Med Rep 12: 8294-8300, 2015.
16. Fitri AR, Pavasant P, Chamni S and Sumrejkanchanakij P: Asiaticoside induces osteogenic differentiation of human periodontal ligament cells through the Wnt pathway. J Periodontol 89: 596-605, 2018.
17. Al-Saeedi FJ, Bitar M and Pariyani S: Effect of asiaticoside on 99mTc-tetrofosmin and 99mTc-sestamibi uptake in MCF-7 cells. J Nucl Med Technol 39: 279-283, 2011.
18. Yingchun L, Huihan W, Rong Z, Guojun Z, Ying Y and Zhuogang L: Antitumor activity of asiaticoside against multiple myeloma drug-resistant cancer cells is mediated by autophagy induction, activation of effector caspases, and inhibition of cell migration, invasion, and STAT-3 signaling pathway. Med Sci Monit 25: 1355-1361, 2019.
19. Huang YH, Zhang SH, Zhen RX, Xu XD and Zhen YS: Asiaticoside inducing apoptosis of tumor cells and enhancing anti-tumor activity of vincristine. Ai Zheng 23: 1599-1604, 2004 (In Chinese).
20. Al-Saeedi FJ: Study of the cytotoxicity of asiaticoside on rats and tumour cells. BMC Cancer 14: 220, 2014.

21. Livak KJ and Schmittgen TD: Analysis of relative gene expression data using real-time quantitative PCR and the 2(-Delta Delta C(T)) method. Methods 25: 402-408, 2001.
22. Perelman A, Wachtel C, Cohen M, Haupt S, Shapiro H and Tzur A: JC-1: Alternative excitation wavelengths facilitate mitochondrial membrane potential cytometry. Cell Death Dis 3: e430, 2012.
23. Soleimani A, Rahmani F, Ferns GA, Ryzhikov M, Avan A and Hassanian SM: Role of the NF-κB signaling pathway in the pathogenesis of colorectal cancer. Gene 726: 144132, 2020.
24. Zhang Q, Lenardo MJ and Baltimore D: 30 Years of NF-κB: A blossoming of relevance to human pathobiology. Cell 168: 37-57, 2017.
25. de Castro Barbosa ML, da Conceicao RA, Fraga AGM, Camarinha BD, de Carvalho Silva GC, Lima AGF, Cardoso EA and de Oliveira Freitas Lione V: NF-kappaB signaling pathway inhibitors as anticancer drug candidates. Anticancer Agents Med Chem 17: 483-490, 2017.
26. Kocyigit A and Guler EM: Curcumin induce DNA damage and apoptosis through generation of reactive oxygen species and reducing mitochondrial membrane potential in melanoma cancer cells. Cell Mol Biol (Noisy-le-grand) 63: 97-105, 2017.
27. Yun X, Rao W, Xiao C and Huang Q: Apoptosis of leukemia K562 and Molt-4 cells induced by emamectin benzoate involving mitochondrial membrane potential loss and intracellular Ca(2+) modulation. Environ Toxicol Pharmacol 52: 280-287, 2017.
28. Yang Y, Zong M, Xu W, Zhang Y, Wang B, Yang M and Tao L: Natural pyrethrins induces apoptosis in human hepatocyte cells via Bax- and Bcl-2-mediated mitochondrial pathway. Chem Biol Interact 262: 38-45, 2017.
29. Tang S, Hu J, Meng Q, Dong X, Wang K, Qi Y, Chu C, Zhang X and Hou L: Daidzein induced apoptosis via down-regulation of Bcl-2/Bax and triggering of the mitochondrial pathway in BGC-823 cells. Cell Biochem Biophys 65: 197-202, 2013.
30. Zhu J, Chen M, Chen N, Ma A, Zhu C, Zhao R, Jiang M, Zhou J, Ye L, Fu H and Zhang X: Glycyrrhetinic acid induces G1phase cell cycle arrest in human nonsmall cell lung cancer cells through endoplasmic reticulum stress pathway. Int J Oncol 46: 981-988, 2015.
31. Bonelli M, Monica SL, Fumarola C and Alfieri R: Multiple effects of CDK4/6 inhibition in cancer: From cell cycle arrest to immunomodulation. Biochem Pharmacol 170: 113676, 2019.
32. He L, Hong G, Zhou L, Zhang J, Fang J, He W, Tickner J, Han X, Zhao L and Xu J: Asiaticoside, a component of *Centella asiatica* attenuates RANKL-induced osteoclastogenesis via NFATc1 and NF-kB signaling pathways. J Cell Physiol 234: 4267-4276, 2019.
33. Yin Z, Yu H, Chen S, Ma C, Ma X, Xu L, Ma Z, Qu R and Ma S: Asiaticoside attenuates diabetes-induced cognition deficits by regulating PI3K/Akt/NF-kB pathway. Behav Brain Res 292: 288-299, 2015.
34. Meshram SN, Paul D, Manne R, Choppara S, Sankaran G, Agrawal Y and Santra MK: FBXO32 activates NF-kB through IkBα degradation in inflammatory and genotoxic stress. Int J Biochem Cell Biol 92: 134-140, 2017.
35. Tsuchiya Y, Osaki K, Kanamoto M, Nakao Y, Takahashi E, Higuchi T and Kamata H: Distinct B subunits of PP2A regulate the NF-kB signalling pathway through dephosphorylation of IKKβ, IkBα and RelA. FEBS Lett 591: 4083-4094, 2017.
36. Hu J, Haseebuddin M, Young M and Colburn NH: Suppression of p65 phosphorylation coincides with inhibition of IkappaBalpha polyubiquitination and degradation. Mol Carcinog 44: 274-284, 2005.
37. Thoms HC, Dunlop MG and Stark LA: p38-mediated inactivation of cyclin D1/cyclin-dependent kinase 4 stimulates nucleolar translocation of RelA and apoptosis in colorectal cancer cells. Cancer Res 67: 1660-1669, 2007.